Ship collision against a 10 MW semi-submersible floating offshore wind turbine

Zhaolong Yu, Jørgen Amdahl

Centre for Autonomous Marine Operations and Systems (AMOS), Norwegian University of Science and Technology (NTNU), Norway

Department of Marine Technology, Norwegian University of Science and Technology (NTNU), Norway.

ABSTRACT: The number of installed offshore wind turbines is continuously expanding worldwide in recent years. Floating offshore wind farms are generally located near the coast close to traffic lanes and are exposed to the risk of collisions from visiting and passing ships. Extreme ship collision events may cause large structural damage, collapse of turbine tower and flooding of compartments, leading to capsizing of turbine platforms.

This paper investigates ship collision responses of a semi-submersible floating offshore wind turbine (FOWT), i.e. the OO-STAR floater with DTU 10 MW blades, using the nonlinear finite element code USFOS. The OO-STAR floater is made of post-tensioned concrete designed by Dr. techn. Olav Olsen. The striking ship is selected to be a modern supply vessel of 7500 tons. Modelling of the FOWT in USFOS is described in detail including the OO-STAR floater, the DTU 10 MW turbine blade, the turbine tower and the mooring system. Eigenmode analysis of the turbine model is performed to verify the modelling. Global collision response analyses of the FOWT were performed in both parked and operating conditions. The ship resistance is modeled as nonlinear springs in USFOS containing force - displacement curves established in LS-DYNA. The results are discussed with respect to global responses of the FOWT and energy absorption.

Keywords: ship collision; floating offshore wind turbine; OO-STAR floater; energy absorption.

1 INTRODUCTION

In order to meet the goals of the Paris Agreement to tackle climate change challenges, the world is undergoing a revolution in global energy system, transitioning fast from classical fossil fuel to clean and decarbonizing energy. Wind power is at the forefront of this evolution. Offshore turbines can utilize the vast free space in the open sea compared to onshore turbines. In addition, the sea environment also provides higher wind speeds for electricity generation and less noise. For regions with shallow water (water depth smaller than 50 m), bottom fixed wind turbines with monopile and jacket foundations are often preferred (refer Fig. 1), because they yield lower overall costs compared to floating wind turbines (DNV-GL, 2020). However, when we move into deep water, where more potential sites can be utilized with richer wind resources, floating wind turbines become advantageous. Floating offshore wind turbines consist of a floater connected to the seabed by mooring lines or tethers. The most common floating foundations are the semi-submersible floater, SPAR and tension leg platform, refer to Fig. 1.

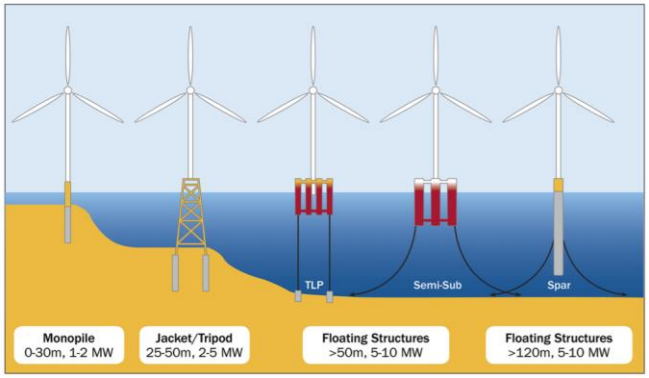

Figure 1 Types of offshore wind turbine foundations (reproduced by European Wind Energy Association (2013), source Principle Power).

Offshore wind farms are often located near the coast close to traffic lanes and are exposed to the risk of collisions from visiting and passing ships due to human errors, unsuccessful avoidance maneuvers or free drifting of vessels following a propulsion damage. The consequence can be catastrophic in extreme conditions with severe structural damage, platform collapse or capsizing, oil leakage, significant

economic loss, and fatalities. It is crucial therefore to gain deep insights into the governing mechanics of ship-offshore turbine collisions, to evaluate the damage stabilities so to design turbine structures against such accidental actions.

Nonlinear finite element methods are powerful tools for simulating ship-offshore wind turbine collisions. For ship collisions with bottom fixed offshore wind turbines, Biehl and Lehmann (2006) studied the behavior of three foundation structures i.e. monopile, tripod, and jacket of offshore wind collided by single (200,000 tons) and double (45,000 tons) hull tankers, bulk carriers (25,000 tons), and container ships (52,000 tons). The ship caused large deformations of the turbine foundations, which were completely torn off in extreme cases. The nacelle and the rotor may fall onto the deck of the striking vessel. The collision loads caused local damage on the ship hull with possible oil leakage. More studies on ship collisions with bottom fixed offshore turbines are found in Bela et al. (2017) and Song et al. (2020) for monopile foundations and Kroondijk (2012) and Le Sourne et al. (2015) for jacket foundations. For ship collision analysis with floating offshore wind turbines, Echeverry et al. (2019) simulated a SPAR type floating offshore wind turbine (FOWT) subjected to collisions from a supply vessel of 5000 tons using LS-DYNA. The vessel motions considering hydrodynamic effects are included. Yu et al. (2021) carried out dynamic response analysis of a 10 MW semi-submersible floating offshore wind turbine subjected to ship collision loads and indicated risk of platform capsizing in extreme cases.

Figure 2. The OO-STAR floating offshore wind turbine design by Dr. techn. Olav Olsen AS

This paper studies dynamic responses of a 10MW sumi-submersible floating offshore wind turbine subjected to collisions from a modern supply vessel. The selected turbine adopts the design from the LIFES50+ project (Pegalajar-Jurado et al., 2015), which consists of the OO-STAR semi-submersible floater designed by Dr. techn. Olav Olsen AS (see Fig. 2), the DTU 10 MW Reference Wind Turbine (RWT) (Bak et al., 2013), and the detailed designs of turbine tower and mooring lines. The ship-FOWT collision analysis is carried out by using the nonlinear finite element software USFOS (Soreide et al., 1999). The results of ship-FOWT collisions are discussed with respect to energy absorption of the ship and the FOWT, and the structural responses.

2 DESCRIPTION OF THE OO-STAR SEMI-SUBMERSIBLE FLOATING WIND TURBINE CONCEPT

2.1 *The OO-STAR floater*

The OO-Star Wind Floater was designed by Dr. techn. Olav Olsen AS in response to the need for innovative solutions for offshore floating winds. The floater is capable of supporting heavy turbines under harsh environmental conditions and can be positioned in areas that are unsuited for bottom-fixed turbines. It is scalable for wind turbine generators of well over 12–15 MW without size limitations related to assembly and installation.

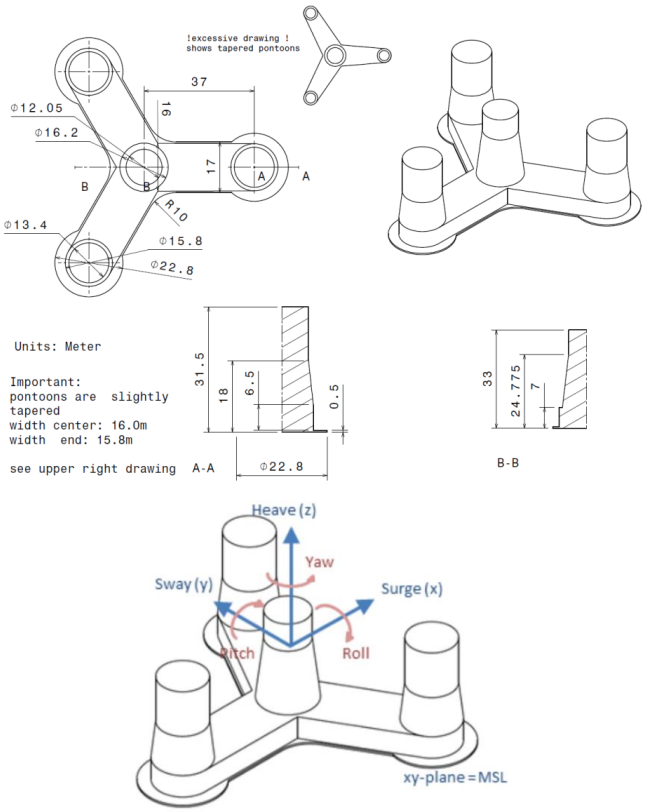

Figure 3. Geometries and the coordinate system of the OO-STAR floater (Pegalajar-Jurado et al., 2015)

The floater consists of a central column and three outer columns mounted on a star-shaped pontoon with a bottom slab. All the columns have a cylindrical upper part and a tapered lower part. The main material is post-tensioned concrete, which yields a higher displaced volume as for steel structures. The geometrical properties of the floater are marked in Fig. 3. The distance between the central column and

the outer column is 37 m. The horizontal pontoon elements connecting the columns have a width of 16 m and a height of 7 m. The slab attached underneath the pontoons has a width of 17 m, adding 0.5 m at each side. The central column has a diameter of 12.05 m at the tower base interface. It has a tapered shape below with a diameter which increases linearly over a length of 17.3 m to 16.2 m at the pontoon interface. The outer columns have a diameter of 13.4 m at the top, and a conical section below, which has a length of 11m with a diameter of 15.8 m at the pontoon interface (Pegalajar-Jurado et al., 2015). The coordinate system on the floater is defined in Fig. 3 with the origin located on the mean surface plane.

2.2 *The mooring system*

The mooring system on the OO-Star Wind Floater is a catenary system with three mooring lines, where the horizontal angle between two chains is 120◦. At each line there is a clumped mass of 50 tons attached. The layout is shown in Fig. 4 (Pegalajar-Jurado et al., 2015). The main parameters of the mooring system are summarized in Table 1.

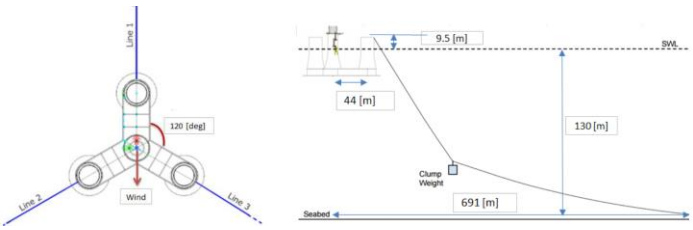

Figure 4. Arrangement of the mooring line system for the OO-STAR floater, from (Pegalajar-Jurado et al., 2015)

Table 1. LIFES50+ OO-Star Floater mooring system properties

Property	LIFES50+ report
Number of lines, [-]	3
Angle between adjacent mooring lines, [deg]	120
Total mass clump weight, [ton]	50
Location of fairleads above MSL, [m]	9.5
Pre-tension, [N]	1.67e+6
Extensional stiffness EA, [N]	1.506e+9
Effective hydraulic diameter of the chain, [m]	0.246
Physical chain diameter [m]	0.137
Hydrodynamic added mass coefficient, [-]	0.8
Hydrodynamic drag coefficient, [-]	2.0

2.3 *DTU 10 MW reference wind turbine*

The DTU 10-MW reference rotor (Bak et al., 2013) is designed as a result of the Light Rotor project by DTU Wind Energy and Vestas. The main objective is to optimize the design of turbine blades to increase the stiffness and overall performance of the rotor, and at the same time the blade weight should be minimized. Some of the key parameters are summarized in Table 2.

Table 2. Key parameters of the DTU 10 MW reference wind turbine

Parameter	**DTU 10MW RWT**
Number of blades	3
Rotor diameter	178.3 m
Hub diameter	5.6 m
Hub Overhang	7.1 m
Rotor mass	227,962 kg
Nacelle mass	446,036 kg
Shaft Tilt Angle	5 deg
Rotor Pre-cone Angle	-2.5 deg
Maximum Rotor Speed	9.6 rpm
Rated Wind Speed	11.4 m/s

3 MODELLING OF THE OO-STAR FLOATING OFFSHORE WIND TURBINE IN USFOS

3.1 *Modelling of the OO-STAR wind turbine*

Modelling of turbine blades and the turbine tower is in accordance with the dimensions by Bak et al. (2013) and Pegalajar-Jurado et al. (2015) in USFOS. Eigenmode analysis of the turbine blade and tower agrees well with target values given in Bak et al. (2013) and Pegalajar-Jurado et al. (2015), demonstrating good modeling accuracy. The OO-STAR floater and the mooring system are modelled according to Pegalajar-Jurado et al. (2015). Decay tests showed good agreement with target natural periods of the platform. Fig. 5 shows the established model in USFOS, and the modelling details and eigenmode analysis can be found in Yu et al. (2021).

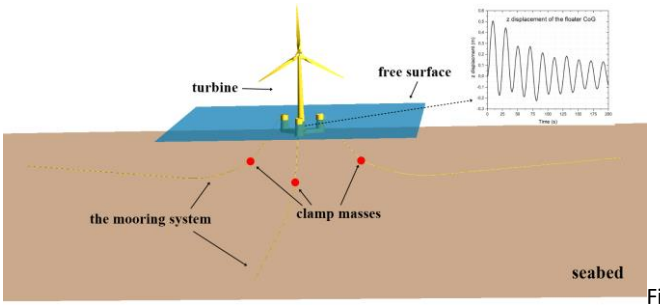

Figure 5. The USFOS model of the OO-STAR floater with DTU 10 MW turbine and the mooring system

3.2 *Hydrodynamic loads*

Buoyancy and gravity loads are applied at the initial stage of analysis. The hydrodynamic inertia forces for the 6DOF motions of the floater are modelled as constant added masses at the turbine COG by activating HYDMASS in USFOS. Infinite frequency added masses from the LIFES50+ D4.5 re-

port (Pegalajar-Jurado et al., 2018) are used. For the drag forces acting on the floater, the Morrison equation is adopted by introducing C_d coefficients. The C_d coefficient is taken from the LIFES50+ D4.5 report (Pegalajar-Jurado et al., 2018), being 0.7 for the floater columns, 2.05 for the pontoons and 10 for the heave plates. For the mooring lines, the Morrison equation is used for both the inertia and drag forces with the mass and drag coefficients being 1.8 and 2.0 respectively according to the LIFES50+ D4.2 report (Pegalajar-Jurado et al., 2015).

3.3 *Wind loads*

Wind thrust forces normal to the rotor plane are crucial for correctly calculating the deflection of blades in operating conditions and are important for the calculation of tower bending moments. In this study, wind thrust forces are calculated by using the HAWC2 software (Larsen and Hansen, 2007) with a rated wind speed of 11.4 m/s. The thrust forces on each section are calculated, and then applied to the corresponding blade elements in USFOS as linearly varying pressure line loads in each element. The resultant thrust force is 1516.7 KN, which agrees well with 1555 KN from the DTU report (Bak et al., 2013) using fully turbulent CFD simulations. The modelled thrust forces on turbine blades in USFOS are shown in Fig. 6. An artificial torque moment is applied at the rotor, and the magnitude is adjusted until the maximum rotor speed of 9.6 rpm is achieved. This corresponds to a nodal velocity of 1 rad/s at the rotor center. After that, the torque moment is reduced to a small value to maintain the constant rotation speed.

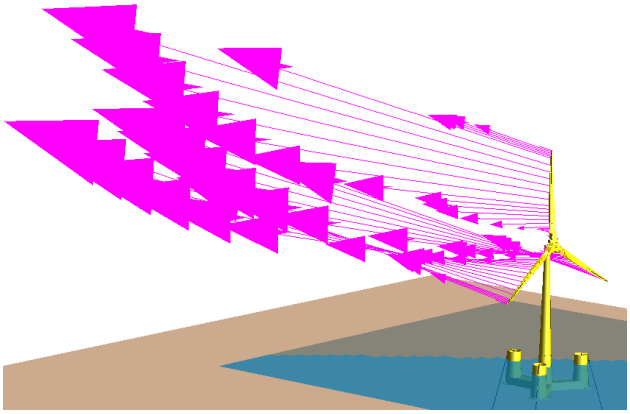

Figure 6. Distribution of wind thrust loads on turbine blades

4 SHIP COLLISION RESPONSE

4.1 *The striking supply vessel*

In this study, the modern UT 745 platform supply vessel with a displacement of 7500 tons is adopted. Fig. 7 (left) shows the finite element model of the bow of the supply vessel. The plate thickness varies from 7 mm for the decks to 12.5 mm in the bulb. The stiffener spacing is about 600 mm with ring stiffeners and breast hooks of approximately 250 × 15 mm in the bulb. The bulbous part is almost cylindrical and is relatively strong. The forecastle protrudes 1.2 m ahead of the bulb. The four-node Belytschko-Lin-Tsay shell element is used with a mesh size of 120 mm in general.

The struck outer concrete column of the floater has a diameter of 13.4 m. The ship bow is fabricated in mild steel, which is assumed to have a yield stress of 275 MPa. The power law material model is used for the mild steel with the power law coefficients K=830 MPa and n=0.24. The RTCL criterion (Tørnqvist, 2003) is adopted for modelling fracture initiation and propagation of steel. The obtained force displacement curves of the ship bow against the rigid column are plotted in Fig. 7(right). The fitted curves approximating the ship resistance will be used as input to USFOS analysis.

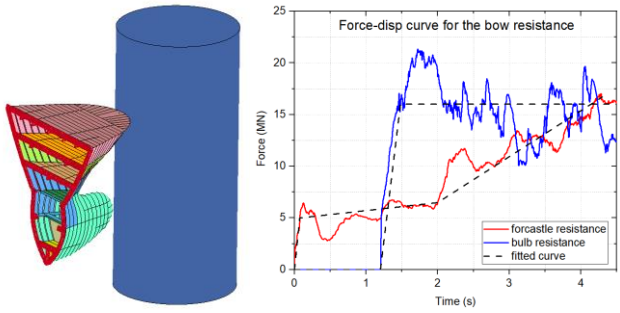

Figure 7. (left) The FE model of the bulbous bow; (right) crushing resistance of the bulbous bow from LS-DYNA simulations. (the dashed line represents the target curve of USFOS input)

For collision analysis with USFOS, a two-spring system is adopted, where the first spring represents ship stiffness and the second models contact. For ship bow collisions, the ship stiffness includes two parts, one for the ship forecastle stiffness on the upper layer and the other for bulb stiffness on the lower layer. The two ship springs are connected by rigid beams (refer to Fig. 8). The ship mass including hydrodynamic added mass is modelled as nodal masses. The contact spring has an “infinite” stiffness in compression to mimic physical contact during collision and zero stiffness in tension to facilitate separation after collision. The ship stiffness is modelled as nonlinear springs, which are defined by force–deformation curves obtained from local collision analysis in LS-DYNA with detailed shell modelling. The Rayleigh type structural damping is adopted in USFOS. The mass proportional damping coefficient is 0.01 and the stiffness proportional damping coefficient is 0.005.

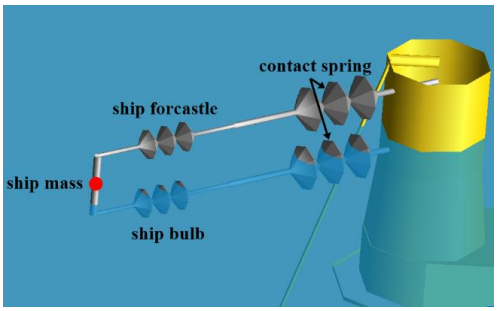

Figure 8. The mass-spring system for ship collisions in USFOS

4.2 *Ship collision with the FOWT in parked condition*

The striking vessel may hit different positions of the FOWT in different directions. The ship impact direction is defined as the angle relative to the rated wind direction (negative *x* direction). Fig. 9 shows several representative collision scenarios with different struck column and impact directions.

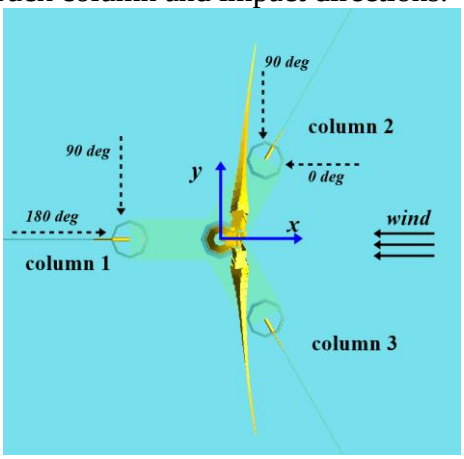

Figure 9. Definition of the ship – FWOT collision scenarios

During weather conditions where the wind speed is below the cut-in speed or the turbine is under maintenance, the FOWT is in parked condition with stationary turbine blades. Hence, structural performance of the FOWT in parked condition under ship impacts is investigated by having stationary blades and no wind loads. Gravity and buoyancy forces are applied at the initial stage of the analysis, and ship collision occurs at 200 s when the system becomes fully stabilized.

Table 3 shows energy absorption of the supply vessel and the FOWT for two representative cases immediately after supply vessel bow collisions. Fig. 10 plots the time evolution of kinetic energy of the collision system in two different cases and the corresponding force displacement curves. The extracted force-displacement curves of the ship bow from USFOS follow well the target curves in Fig. 7, demonstrating correct implementation of the ship resistance model. Fig. 11 plots characteristic motions of the supply vessel and the FOWT during and after collisions. For supply vessel bow collisions, a collision velocity of 3 m/s for the selected vessel yields a total energy of 37.1 MJ considering hydrodynamic effects. The supply bow deforms significantly in collisions and absorb considerable energy. Little kinetic energy remains in the supply vessel after collision in general. For the cases *column1-180deg-supply vessel bow*, the FOWT response is dominated by translatory motions. For the cases *column1-90deg-supply vessel bow*, multiple impacts are observed from the velocity plots in Fig. 11, where the yaw and sway motions of the FOWT dominate. A small part of the total energy may be dissipated through vibration of the tower, structural damping, hydrodynamic damping and the mooring system.

Table 3. Energy dissipation of the supply vessel and the parked FOWT immediately after collision

Case	column1-180-bow	column1-90-bow
Total energy	37.1 MJ	37.1 MJ
supply vessel strain energy	Forecastle 12.7 MJ Bulb 14.3 MJ	Forecastle 11.3 Bulb 9.7
supply vessel kinetic energy after first collision	0.1 MJ	0.7 MJ
Main motion energy of the FOWT after collision	8.7 MJ, Including: surge motion 6.3 MJ pitch motion 1.3 MJ top structure energy 1.1 MJ	12.8 MJ, Including: sway motion 4.1 MJ Yaw motion 6.7 MJ Roll motion 1.0 MJ top structure energy 1.0 MJ
Others	1.4 MJ	3.3 MJ

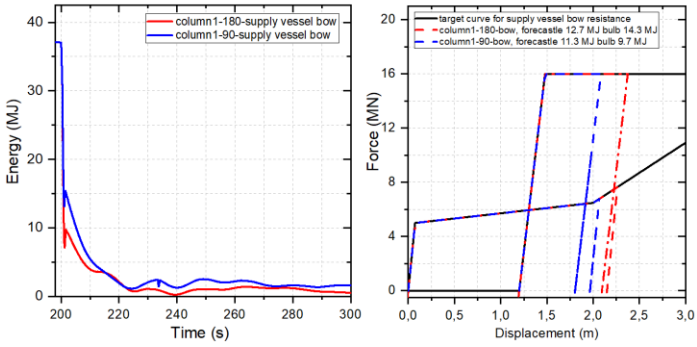

Figure 10. (left) Kinetic energy of the supply vessel bow-parked FWOT system during and after collision; (right) Force-displacement curves of the supply vessel forecastle and bulb in collisions

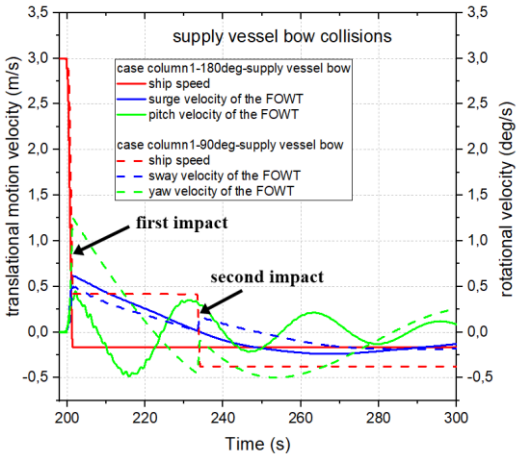

Figure 11. Motions of the ship and the parked OO-STAR floating turbine during and after supply vessel bow collisions

4.3 *Ship collision with the FOWT in operative condition*

For operating wind turbines with rotating blades and wind thrust forces, the collision risk may potentially be more serious. In the collision analysis with the operating FOWT, buoyancy and gravitational loads are applied at the initial stage. Wind thrust loads and moments for blade rotation are applied at 70 s, and the FOWT is then gradually pushed away to a displacement of 33 m (refer to Fig. 12) when the wind thrust is balanced by the mooring system. Under the action of wind thrust at the rated wind speed, the FOWT has a steady negative pitch angle of 5.8° in operating conditions. Ship collision is assumed to occur at 400 s after stabilization of the system.

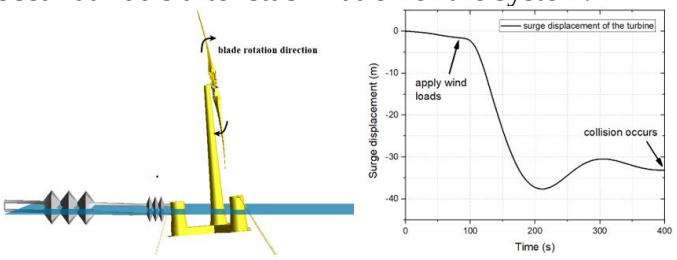

Figure 12. Pitch motion of the OO-STAR floating turbine after stabilization of the system in operating conditions

Fig. 13 plots time evolution of kinetic energy of the collision system with operating turbines in different collision cases from the supply vessel bow, and the corresponding force displacement curves. Energy absorption of the supply vessel and the OO-STAR floating wind turbine for two representative cases immediately after collisions is summarized in Table 4. Fig. 14 plots velocities of the characteristic motions of the supply vessel and the turbine during and after collisions.

Table 4. Energy dissipation of the supply vessel and the parked FOWT immediately after collision

Case	column1-180deg-supply vessel bow	column2-0deg-supply vessel bow
Total energy	37.1 MJ	37.1 MJ
Ship deformation energy	Forecastle 17.5 MJ Bulb 9.7 MJ	Forecastle 8.0 Bulb 14.3
Ship kinetic energy after first impact	0.2 MJ	0.3 MJ
Main motion energy of the FOWT after collision	8.4 MJ, Including: surge motion 6.7 MJ pitch motion 0.7 MJ top structure energy 1 MJ	11.8 MJ, Including: surge motion 4.3 MJ yaw motion 5.7 MJ Pitch motion 0.9 MJ top structure energy 0.9 MJ
Others	1.3 MJ	2.7 MJ

The results show that for supply vessel bow collisions, the distribution of energy absorption in the forecastle and the bulb is quite different with the turbine in parked condition because of the turbine pitch motion under wind thrust. Fig. 15 plots an example of the temporal evolution of the pitch motion for the case *column1-180deg-supply vessel bow*. With the buoyancy and gravity loads applied, the turbine has a small initial pitch angle of about 0.7°due to offset of the rotor. When wind loads are applied, the turbine reaches a steady pitch angle of about -5.8° in operation conditions. This changes the relative distance of the bulb and the forecastle to the platform, yielding different energy distribution in the forecastle and bulb compared to that in parked condition. More energy goes into the bulb when the collision is in line with the wind direction. Conversely, when the supply vessel collides from the opposite wind direction, the ship forecastle dissipates more energy.

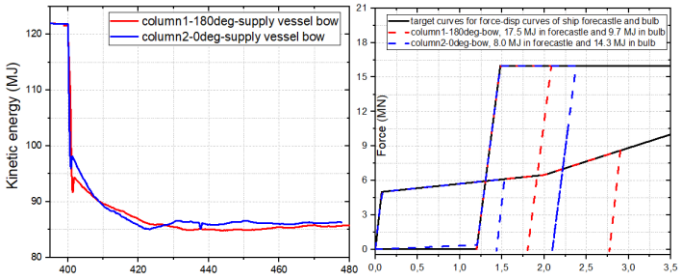

Figure 13. (left) Kinetic energy of the supply vessel bow-operating FWOT system during and after collision; (right) Force-displacement curves of the supply vessel bow in collisions

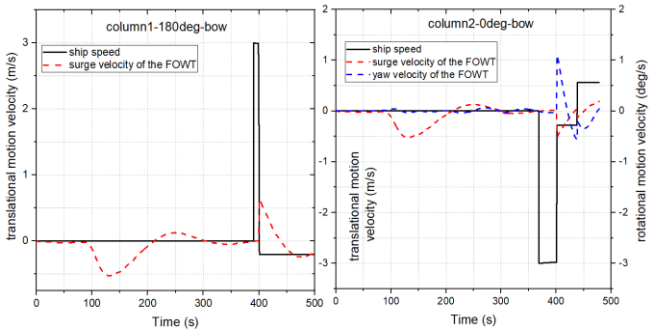

Figure 14. Motions of the supply vessel and the operating OO-STAR turbine during and after bow collisions for two different cases

Generally, the energy absorption modes do not differ much from collisions with the turbine in parked conditions. The supply vessel bow deforms significantly and absorb considerable energy, i.e. 22.3 - 27.2 MJ for the ship bow from Table 4. Limited kinetic energy remains in the ship after collision. The FOWT dissipates energy mainly through motions of turbine floater and the top structure. The rest of the energy is dissipated through vibration of the tower, structural damping, hydrodynamic damping and the mooring system. The energy dissipated by vibrations of the tower is small in general.

It is common industrial practice for designing floating wind turbines to set an operational limit for the tower-top axial acceleration, normally in the range of 0.2–0.3 g, which is typically understood to be related to the safety of delicate mechanical and electrical equipment in the nacelle. Fig. 16 plots nacelle accelerations for the OO-STAR floating turbine in operative conditions subjected to collisions from the supply vessel bow. The selected scenarios

represent ship collisions along the wind direction and opposite to the wind direction, respectively. The plots show that the nacelle accelerations exceed the maximum allowable operation limit of 0.2 g. It is noted that nacelle accelerations are somewhat reduced when the vessel hits from the opposite wind direction and are magnified to some extent for collisions in line with the wind direction.

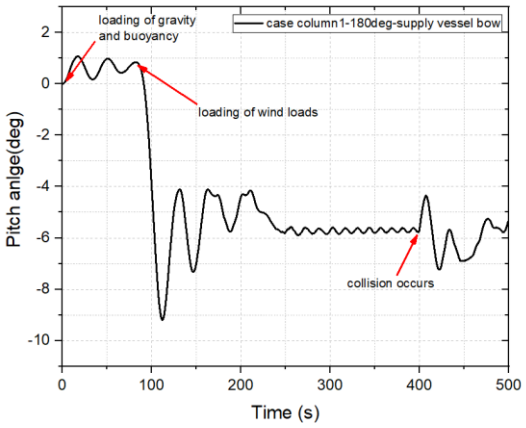

Figure. 15. Pitch angle of the operating OO-STAR turbine for case column1-180deg-supply vessel bow

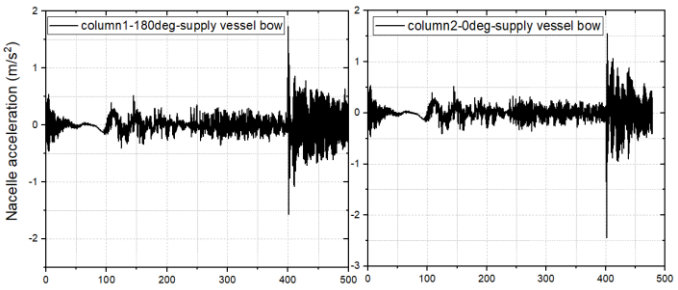

Figure 16. Acceleration of the turbine nacelle during and after supply vessel bow collisions in operating conditions

The maximum blade tip deflection is an important design parameter, and the blades must be kept at a safe distance from the turbine tower. For that matter, the blades often have a prebend, the rotor has a precone angle and the shaft is tilted. All these effects increase the tower clearance. It is crucial to monitor the clearance during an accidental ship collision as the consequence of an impact between the turbine tower and the blade can be severe, causing repair downtime and economic losses.

The tower clearance can be reduced by bending and vibration of the turbine blades and bending of the tower. Fig. 17 plots the displacement of the blade tip relative to its undeformed position for two representative collision cases from supply vessel bow, and the cases are considered to give the worst conditions of the tower clearance. The turbine blade yields a deflection of about 6.8 m at the rated wind speed of 11.4 m/s. When collision occurs, the turbine blade starts to vibrate, yielding a maximum blade tip deflection of 8.25 m for supply vessel bow collision from the opposite wind direction and 8.58 m for bow collision from in line with the wind direction. This indicates that it is more dangerous for the reduction of tower clearance when the vessel direction aligns with the wind direction. Considering a total tower clearance of 16.5 m, the studied FOWT has sufficient margins to avoid collision between blades and the tower for supply vessel collisions.

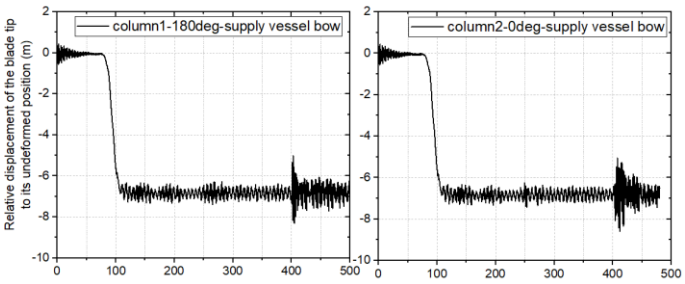

Figure 17. Displacement of the blade tip relative to its undeformed state for two different cases.

5 CONCLUSIONS

This paper presents numerical modelling and dynamic response analysis of a 10 MW semi-submersible floating offshore wind turbine subjected to ship collision loads from a supply vessel bow. Wind turbines in both parked and operative conditions are considered. The studied semi-submersible floating wind turbine is in general safe with respect to global motions, tower bending, blade tower clearance and mooring line forces when it is subjected to collision with a ship similar to a modern supply vessel with an initial kinetic energy of 37 MJ for bow collisions. The nacelle accelerations, however, exceed the allowable operational limit and may damage the delicate mechanical and electric equipment inside the nacelle.

It is generally more critical when ship collision occurs on an operating floating wind turbine, and the worst case is when the vessel strikes from the opposite of the wind direction. Wind thrust loads on turbine blades will induce a negative pitch angle of the platform. In addition, the wind loads also increase tower bending moments and nacelle accelerations, and therefore increase the risk of tower buckling and exceedance of the nacelle operational limits.

ACKNOWLEDGEMENT

The authors gratefully acknowledge the financial support by Research Council of Norway via the Centers of Excellence funding scheme, project number 223254 – NTNU AMOS. The authors would also like to thank the support from high performance computation resources from the Norwegian national e-infrastructures, Project NN9585K - Accidental actions on strait crossings and offshore platforms.

REFERENCES

Dr.techn. Olav Olsen AS URL http://www.olavolsen.no/.

2013. European Wind Energy Association: Deep Water: The Next Step for Offshore Wind Energy. *Brussels, Belgium: A report by the European Wind Energy Association*.

BAK, C., ZAHLE, F., BITSCHE, R., KIM, T., YDE, A., HENRIKSEN, L. C., HANSEN, M. H., BLASQUES, J. P. A. A., GAUNAA, M. & NATARAJAN, A. The DTU 10-MW reference wind turbine. Danish Wind Power Research 2013, 2013.

BELA, A., LE SOURNE, H., BULDGEN, L. & RIGO, P. 2017. Ship collision analysis on offshore wind turbine monopile foundations. *Marine Structures*, 51**,** 220-241.

BIEHL, F. & LEHMANN, E. 2006. Collisions of ships with offshore wind turbines: Calculation and risk evaluation. *Offshore Wind Energy*. Springer.

DNV-GL 2020. FLOATING WIND: THE POWER TO COMMERCIALIZE Insights and reasons for confidence. *DNV report*.

ECHEVERRY, S., MÁRQUEZ, L., RIGO, P. & LE SOURNE, H. Numerical crashworthiness analysis of a spar floating offshore wind turbine impacted by a ship. Developments in the Collision and Grounding of Ships and Offshore Structures: Proceedings of the 8th International Conference on Collision and Grounding of Ships and Offshore Structures (ICCGS 2019), 21-23 October, 2019, Lisbon, Portugal, 2019. CRC Press, 85.

KROONDIJK, R. 2012. *High energy ship collisions with bottom supported offshore wind turbines*. Institutt for marin teknikk.

LARSEN, T. J. & HANSEN, A. M. 2007. How 2 HAWC2, the user's manual. *December 2007*.

LE SOURNE, H., BARRERA, A. & MALIAKEL, J. B. 2015. Numerical crashworthiness analysis of an offshore wind turbine jacket impacted by a ship. *Journal of Marine Science and Technology*, 23**,** 694-704.

PEGALAJAR-JURADO, A., MADSEN, F., BORG, M. & BREDMOSE, H. 2015. Qualification of innovative floating substructures for 10MW wind turbines and water depths greater than 50m. *LIFES50+ project report*.

PEGALAJAR-JURADO, A., MADSEN, F., BORG, M. & BREDMOSE, H. 2018. State - of - the - art models for the two LIFES 50+ 10MW floater concepts. tech. rep.

SONG, M., JIANG, Z. & YUAN, W. 2020. Numerical and analytical analysis of a monopile-supported offshore wind turbine under ship impacts. *Renewable Energy*.

SOREIDE, T., AMDAHL, J., EBERG, E., HELLAN, O. & HALMÅS, T. 1999. USFOS–a computer program for progressive collapse analysis of steel offshore structures. *Theory Manual. SINTEF Report STF71 F*, 88038.

TØRNQVIST, R. 2003. *Design of crashworthy ship structures*. Technical University of Denmark Kgns Lyngby,, Denmark.

YU, Z., AMDAHL, J., RYPESTØL, M. & CHENG, Z. 2021. Numerical modelling and dynamic response analysis of a 10 MW semi-submersible floating offshore wind turbine subjected to ship collision loads. *submitted to journal*.